DOI: 10.1002/chem.200600916

Long-Range-Distance NMR Effects in a Protein Labeled with a Lanthanide–DOTA Chelate

Monica D. Vlasie,[a, d] Clara Comuzzi,[a, b, d] Adrianus M. C. H. van den Nieuwendijk,[a] Miguel Prudêncio,[a, c] Mark Overhand,[a] and Marcellus Ubbink*[a]

Abstract: A two-thiol reactive lanthanide–DOTA (1,4,7,10-tetraazacyclododecane-*N*,*N*′,*N*″,*N*‴-tetraacetic acid) chelate, CLaNP-3 (CLaNP = caged lanthanide NMR probe), was synthesized for the rigid attachment to cysteine groups on a protein surface, and used to obtain long-range-distance information from the $\{^{15}N,^{1}H\}$ HSQC spectra of the protein–lanthanide complex. The DOTA ring exhibits several isomers that are in exchange; however, single resonances were observed for most amide groups in the protein, allowing determination of a single, apparent magnetic-susceptibility tensor. Pseudocontact shifts caused by Yb-containing CLaNP-3 were observed for atoms at 15–35 Å from the metal. By using Gd-containing CLaNP-3, relaxation effects were observed, allowing distances up to 30 Å from the paramagnetic center to be determined accurately. Similar results were obtained with a Gd–DTPA (diethylene-triaminepentaacetic acid) chelate, CLaNP-1, bound in the same bidentate manner to the protein. This study demonstrates that bidentate attachment of a paramagnetic probe enables determination of long-range distances.

Keywords: cage compounds · lanthanides · NMR spectroscopy · paramagnetic relaxation · pseudocontact shifts

Introduction

Long-range-distance information is required for solution structure determination of flexible molecules, such as nucleic acids or multidomain proteins, as well as for complexes of macromolecules.

Paramagnetic NMR effects, such as pseudocontact shifts (PCS), paramagnetic relaxation enhancement (PRE), and paramagnetic cross-correlated relaxation, are caused by the presence of unpaired electrons and are felt by the nuclear spins situated up to tens of Ångströms away. These effects are well understood and provide useful tools in structure determination.

Paramagnetic effects can be used in protein NMR analysis by addition of transition metals,[1,2] lanthanide ions,[3,4] lanthanide chelates,[5–10] stable radicals, such as 2,2,6,6-tetramethylpiperidine-1-oxyl (TEMPO),[11–16] or dioxygen,[17] to decrease the signal overlap of the resonances observed, to probe the molecular surface of these large molecules, or to align macromolecules for residual dipolar-coupling measurements.

A wealth of structural information was obtained from the paramagnetic NMR on proteins that contain a paramagnetic metal, or in which a diamagnetic metal could be substituted for a paramagnetic one.[18–34] As was first demonstrated for the cytochrome *f*–plastocyanin complex,[35–38] paramagnetic effects can also be used for structure determination of protein complexes.[39] Metal substitution can also be used effectively for this purpose.[40] Although there are quite a few examples for which a paramagnetic metal exists or can be engineered inside the core of a protein, there are numerous others for which this is not possible. This disadvantage can be eliminated by the construction of paramagnetic probes

[a] Dr. M. D. Vlasie, Dr. C. Comuzzi, A. M. C. H. van den Nieuwendijk, Dr. M. Prudêncio, Dr. M. Overhand, Dr. M. Ubbink
Leiden Institute of Chemistry
Gorlaeus Laboratories Leiden University
P.O. Box 9502, 2300 RA Leiden (The Netherlands)
Fax: (+31) 71-5274-349
E-mail: m.ubbink@chem.leidenuniv.nl

[b] Dr. C. Comuzzi
On leave from Dipartimento di Scienze e Tecnologie Chimiche
Via del Cotonificio 108, Universita' di Udine 33100 Udine (Italy)

[c] Dr. M. Prudêncio
Present address: Unidade de Malária
Instituto de Medicina Molecular, Universidade de Lisboa
1649–028 Lisboa (Portugal)

[d] Dr. M. D. Vlasie, Dr. C. Comuzzi
These authors contributed equally to this work.

Supporting information for this article is available on the WWW under http://www.chemeurj.org/ or from the author.

for covalent attachment to the protein. One possibility is to use N- or C-terminal fusion peptides engineered to bind a paramagnetic metal for co-expression with the protein of interest, however, this limits the choice for the location of the metal.[41–45]

Another possibility is to attach site-specific probes onto the surface of the macromolecule by chemical methods. In this way, different paramagnetic centers, such as nitroxide spin labels,[46–54] coordinated divalent metals,[55–58] and lanthanide chelates,[59–64] were created and can be used for structure refinement. Lanthanides are strong paramagnetic agents and, therefore, particularly useful in providing a range of effects that can be fine-tuned over large distances. Most lanthanide chelates were synthesized and specifically attached to the proteins through one reactive arm. Depending on the number of bonds between the lanthanide and the protein backbone, such probes can have considerable flexibility. In our laboratory, a paramagnetic probe was designed [60] with two attachment points on the protein surface and, consequently, reduced mobility. A drawback of this probe is the presence of several isomeric forms of the lanthanide chelate that cause several resonances for a spin that experiences a PCS.

PCS values can provide long-range-distance information, of 5–40 Å from the paramagnetic center,[20] by exploiting the magnetic-anisotropy properties of different lanthanides with fast electron-spin relaxation. The magnitude of the PCS is proportional to the inverse cube of the distance, providing quite a sensitive tool for obtaining distance restraints. The anisotropic nature of the PCS, described by the magnetic-susceptibility tensor (χ), requires the metal to exhibit a single type of coordination. In particular, Ln complexes often show isomers that are in exchange, which result in multiple χ tensors and, thus, multiple resonances for a nucleus.[59,60] In contrast, PRE are isotropic to a good approximation and are proportional to the inverse sixth power of the distance between the paramagnetic metal ion and the nucleus observed. Among the lanthanides, Gd^{3+} is a useful PRE agent because of its long electronic relaxation time.

Here, we report the synthesis and characterization of a DOTA-based (DOTA = 1,4,7,10-tetraazacyclododecane-*N*,*N*′,*N*″,*N*‴-tetraacetic acid) lanthanide chelate that is attached to a protein through two disulfide bridges. Single resonances were obtained for most of the residues in the Yb^{3+} chelate and the observed PCS can be fitted well with a single apparent χ tensor. Furthermore, the Gd^{3+} chelate of this probe, as well as of an earlier DTPA-derived (DTPA = diethylene-triaminepentaacetic acid) form,[60] are shown to produce PRE with reliable distance dependencies in the range of 20–30 Å, making them useful spectroscopic tools for macromolecular structure determination.

Results and Discussion

Synthesis and properties of the caged lanthanide NMR probe (CLaNP) molecule: The strategy to synthesize the modified DOTA derivative **3b**, capable of ligation to two proximate engineered cysteine residues of a protein, is depicted in Scheme 1. Commercially available cyclen was transformed in three synthetic steps[65] to obtain the bis(*tert*-butyloxycarbonylmethylene) derivative, compound **1**. Reaction of **1** with benzyl bromoacetate in the presence of potassium carbonate gave compound **2** in moderate yield after silica-gel column chromatography. Liberation of two carboxylic acid functionalities was accomplished by removal of the two benzyl groups of **2** by using a catalytic amount of palladium on carbon under a hydrogen atmosphere. The resulting dicarboxylic acid intermediate was coupled to 2-(aminoethyl)methanethiosulfonate with the aid of 1-(3-dimethylaminopropyl)-3-ethylcarbodiimide-HCl (EDCI) to provide compound **3a** in 26% yield over the two steps after purification by HPLC. Removal of the *tert*-butyl ester groups was accomplished with 33% trifluoroacetic acid in di-

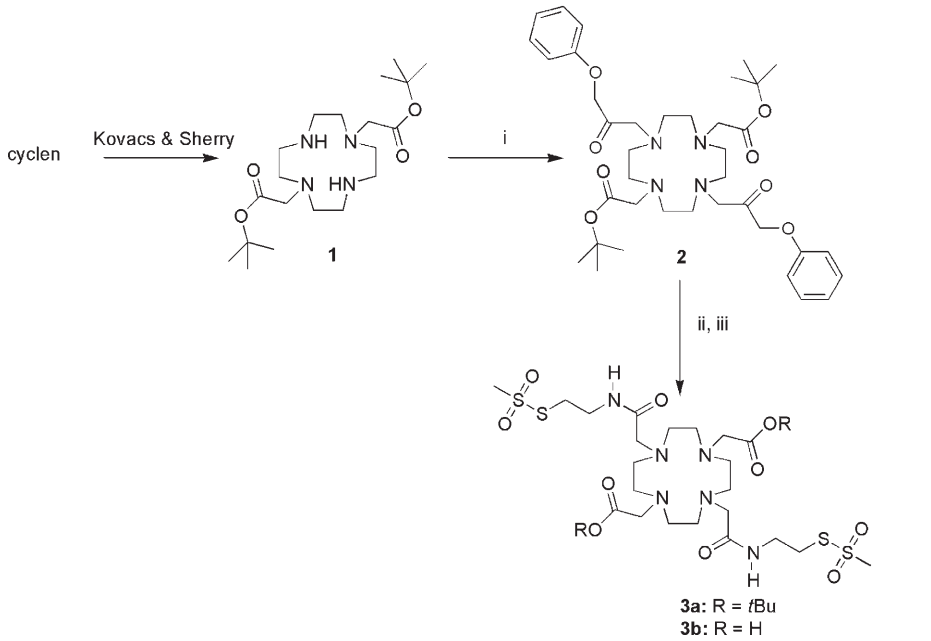

Scheme 1. Synthesis of the CLaNP-3 molecule: i) $BrCH_2CO_2Bn$, K_2CO_3/MeCN; ii) Pd–C/H_2, EtOH; iii) EDCI, $H_2NCH_2CH_2SSO_2CH_3$, TFA.

chloromethane to give compound **3b** in 36% yield after HPLC purification.

Attachment of the CLaNP molecules to E51C/E54C-Paz: The CLaNP molecules (Figure 1A and B) were attached to

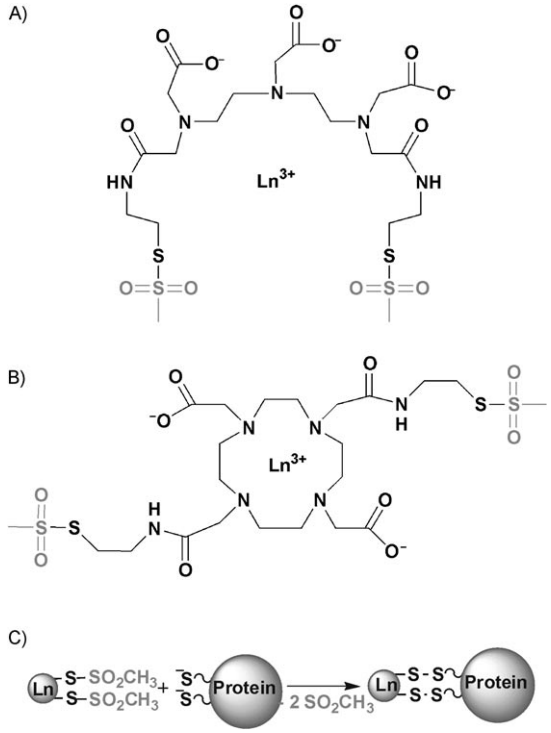

Figure 1. Chemical structures of A) the bis(MTS) derivative of DTPA, CLaNP-1,[60] and B) the bis(MTS) derivative of DOTA, CLaNP-3. The leaving groups of the probe molecule are shown in gray. C) Schematic representation of the attachment reaction between the probe molecule and the cysteine residues of the protein.

the test protein in a bidentate fashion through two engineered cysteine residues (Figure 1C), limiting the rotational freedom of the lanthanide ion with respect to the protein. We found that attachment of the bidentate CLaNP molecules does not depend critically on the position or distance of the two Cys residues. Various proteins were tagged successfully with Cys–Cys CB distances within the range of 5–10 Å (not shown). The minimal distance between the sulfur atoms should be large enough to avoid intramolecular disulfide-bridge formation. Generally, exposed polar residues are selected for mutation to minimize effects on protein structure.

A variant of pseudoazurin (Paz) with mutations E51C and E54C[60] was used to test the effects of the CLaNP molecules. Paz is a small copper-containing protein (14 kDa) and does not contain any exposed cysteine residues. The only cysteine in the wild-type protein provides one of the four ligands to the copper.

Attachment of the CLaNP-3 molecule to the protein was checked by mass spectrometry. Mass spectroscopy analysis (TOF, ES+) revealed a mass of 14316 ± 2 Da for the ^{Yb}CLaNP-3 bound to ^{15}N-Paz, consistent with binding of the probe to the protein through both reactive arms (expected mass 14317 Da for a 99% incorporation of ^{15}N in ^{Yb}CLaNP-3–Paz). The attachment of the CLaNP-1 molecule to Paz in a bidentate manner was confirmed previously.[60]

The $\{^{15}N,^{1}H\}$ HSQC spectra of the ^{Y}CLaNP-1, the diamagnetic control probe, bound to this mutant exhibited only small chemical-shift perturbations for several residues in the neighborhood of the attachment site, relative to the wild-type Paz spectra, however the remaining amide resonances remained unaffected. The overall similarity between these two structures was also confirmed by X-ray crystallography results.[60] The differences in chemical shift between ^{Y}ClaNP-1 and ^{Y}CLaNP-3 bound to this Paz mutant, for most of the amide protons, are less than 0.02 ppm (see Figure S1 in the Supporting Information). This indicates that CLaNP-3 binding also does not affect the overall three-dimensional structure of Paz. Notably, similar to the case of CLaNP-1 bound to this mutant Paz, the resonances for C51, C54, and the residues in their immediate vicinity are not observed in the HSQC spectra of the diamagnetic sample. The disappearance of these signals might be attributed to line broadening due to a slow exchange process in the residues on the loop to which the CLaNP is attached.

Pseudocontact shifts caused by ^{Yb}CLaNP-3: Lanthanide-substituted DOTA exhibits several isomers in solution, differing in conformation and water coordination.[66] The Ln–DOTA conformers represent two enantiomeric pairs of diastereoisomers. Two sets of peaks are generally observed in NMR spectra due to slow conversion of the DOTA isomers.[67,68] In the HSQC spectra of the diamagnetic ^{Y}CLaNP-3–Paz, single peaks are observed for all residues, indicating that the protein amide groups are too far from the probe to sense possible exchange processes. In the case of the paramagnetic Paz–^{Yb}CLaNP-3, nearly all peaks exhibit changes in chemical shift that are of about the same size in the proton and nitrogen dimensions. This is a hallmark of PCS because the shifts are independent of the type of nucleus when expressed in ppm. Most residues show single peaks, some exhibit a small splitting in the ^{1}H dimension only, and some amides close to the probe (<18 Å) are not observed at all (Figure 2A). We attribute these observations to the DOTA isomers, as will be discussed below.

Due to the attachment of CLaNP-3 to the protein through its two reactive arms, the symmetry in the coordination complex is altered, resulting in four distinguishable isomers, giving rise to four possible χ tensors. The peaks that are split in the ^{1}H dimension represent the effects of two χ tensors, caused by exchange between two conformers of the CLaNP molecule.[69] The fact that the splittings are small and even absent for most peaks suggests that these two conformers have χ tensors with similar orientations.

Resonances due to the amide group at >10 Å from the metal should be observable, in agreement with the results obtained with ^{Yb}CLaNP-1–Paz.[60] The absence of resonances from amides close (<18 Å) to the metal cannot be caused

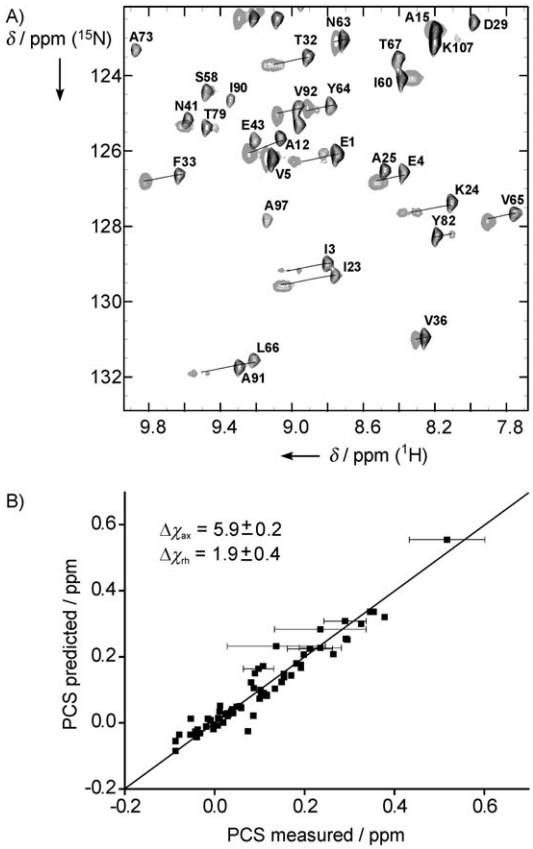

Figure 2. Pseudocontact shifts of ^{Yb}CLaNP-3 bound to Paz: A) a section of the overlaid {^{15}N,^{1}H} HSQC spectra of ^{Yb}CLaNP-3–Paz–Cu(I) (gray) and ^{Y}CLaNP-3–Paz–Cu(I) (black). Some of the shifted amide resonances are connected by lines with slopes close to unity to indicate the pseudocontact nature of the shift; B) correlation between measured and predicted PCS for 70 amide protons of Paz. Predicted PCS were back-calculated with the optimized apparent χ tensor. The axial and rhombic contributions of the $\Delta\chi$ are given in units of 10^{-32} m^3.

by the paramagnetic relaxation effects. Neither can it be attributed to exchange effects in the protein due to probe attachment, because the resonances are clearly observed in the diamagnetic control, ^{Y}CLaNP-3–Paz. We suggest that a second exchange process in the DOTA part of CLaNP-3 results in doubling of the resonances. If the exchange between these forms is on the order of several hundred per second, the resonances of amides with two very different PCS will be broadened; however, those with only slightly different PCS will show a single, average resonance. Thus, the signals of amides close to the metal will mostly broaden out, whereas those from more-distant amides will show a single resonance. The published data[70,71] are contradictory with regard to the sizes of the exchange rates of the various interconversions. Therefore, no attempt will be made here to assign the two proposed exchange processes to specific conformer isomerizations.

To establish whether the observed PCS could be used for structural calculations, the data were fitted to Equation (1) (see Experimental Section), yielding a good correlation for observed versus predicted PCS with a single apparent tensor, χ^{app} (Figure 2B). These results indicate that CLaNP-3 can provide useful PCS data, despite its exchange behavior.

Paramagnetic relaxation enhancement (PRE) caused by ^{Gd}CLaNP molecules: Unlike other lanthanides, Gd^{3+} has a slow electronic relaxation rate, causing strong relaxation effects on surrounding nuclear spins. These effects are isotropic to a good approximation[72] and are, therefore, independent of the presence of more than one isoform of the CLaNP molecules. The PRE falls off with the sixth power of distance from the Gd^{3+} [Eq. (3), Experimental Section], making it a very sensitive tool for distance measurements. The Gd^{3+} ion does not cause significant PCS.

To test the usefulness of PRE caused by Gd^{3+}, the effects of ^{Gd}CLaNP molecules on Paz amide protons were determined by acquiring {^{15}N,^{1}H} HSQC spectra of ^{Gd}CLaNP-1 and ^{Gd}CLaNP-3 bound to the ^{15}N-labeled Paz. The intensities were compared with those in control spectra of ^{Y}CLaNP–Paz. Large intensity differences were observed for numerous peaks. Figures 3A and B show the peak-intensity ratios of ^{Y}CLaNP-1–Paz to ^{Gd}CLaNP-1–Paz and of ^{Y}CLaNP-3–Paz to ^{Gd}CLaNP-3–Paz, respectively, for all Paz residues observed. The residues that appear unaffected by the Gd^{3+} ion show an intensity ratio of 1. For residues ob-

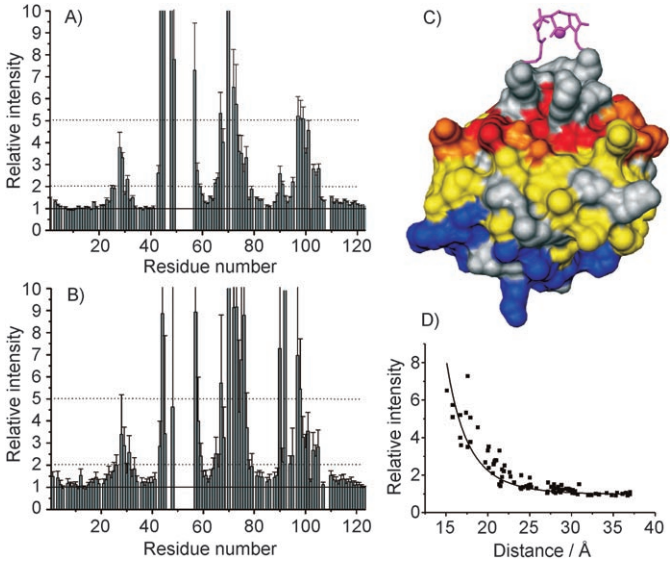

Figure 3. Relaxation enhancements of ^{Gd}CLaNP-1 and ^{Gd}CLaNP-3 bound to Paz. Relative intensities of the diamagnetic versus paramagnetic sample for all observed residues in the NMR experiment: A) ratio of ^{Y}CLaNP-1–Paz intensities to ^{Gd}CLaNP-1–Paz intensities; B) ratio of ^{Y}CLaNP-3–Paz intensities to ^{Gd}CLaNP-3–Paz intensities. Error bars were calculated by using the background intensity. C) Map of the relaxation effects caused by the Gd^{3+} on Paz. A decrease in intensity of the amide resonances in ^{Gd}CLaNP-1–Paz versus ^{Y}CLaNP-1–Paz of more than five times is shown in red, between five and two times in orange, between two and 1.2 times in yellow, and below 1.2 times in blue. The five- and two-fold borders are marked in panels A and B by dotted lines. The unassigned and Pro residues are gray. The CLaNP-1 molecule with the bound Y^{3+} is purple. The structure of the ^{Y}CLaNP-1–Paz was taken from the PDB entry 1PY0.[60] D) Relative intensity (I^{dia}/I^{para}) for CLaNP-1–Paz residues versus the distance from the Gd ion to the amide protons. The solid line represents a fit of the data by using the equation $y=1+bx^{-6}$.

served in the diamagnetic sample that had disappeared in the paramagnetic one, the noise-level intensity was used to calculate the minimal ratio of intensities in the two forms. The broadening effects of the Paz resonances caused by the Gd^{3+} in the CLaNP-1 protein complex were then mapped onto the crystal structure of CLaNP-1–Paz (Figure 3C). A clear distance-dependent decrease in intensity of the Paz peaks with respect to the lanthanide is apparent (Figure 3D).

Modeling the position of the lanthanide with respect to the protein by using NMR-derived distances as restraints: To quantify the distances from the HSQC peak intensities, the R_2^{para} values were determined by using Equation (2) (Experimental Section).[46] The use of intensity ratios yields R_2^{para} values that are slightly less precise than those obtained through direct R_2 determination. However, it has been demonstrated that other approximations concerning PRE distance determination introduce larger errors.[49,51] Furthermore, this approach is simpler and is also applicable to larger protein complexes. According to Equation (3), at the magnetic field used, R_2^{para} is proportional to the correlation time τ_c. The latter depends on the electronic relaxation time of the Gd^{3+} ion (τ_s), the rotational correlation time of the metal–proton vector (τ_r), and possible exchange processes (τ_M). The contribution of the τ_M is likely to be relatively small. Both τ_s and τ_r are expected to be in the low-nanosecond range. To obtain τ_c, the R_2^{para} values were fitted to Equation (3) by using the crystal structure of Paz–^{Y}CLaNP-1 as a reference for the distances, and with τ_c as the only variable. Values of 4.0 ± 0.9 and 5.9 ± 1.2 ns were obtained for ^{Gd}CLaNP-1–Paz and ^{Gd}CLaNP-3–Paz, respectively, indicating that within the error, the τ_c values are the same.

The NMR-derived distances obtained with these τ_c values were used to optimize the position of the Gd ion relative to Paz for both CLaNP molecules. Restrained energy minimization by using only the distance information placed the Gd^{3+} ion at 2.4 Å and 4.8 Å from the lanthanide position observed in the crystal structure of Paz–CLaNP-1[60] for ^{Gd}CLaNP-1–Paz and ^{Gd}CLaNP-3–Paz, respectively (Figure 4A). Due to dependence on the sixth power of the distance, the predicted distances are not very sensitive to errors in τ_c. A 50% higher or lower value for the τ_c led to an optimized position of the Gd ion that differed by 1.3 Å from the one obtained above.

These calculations suggest that the solution position of the lanthanide in CLaNP-1 is similar to that observed in the crystal. The lanthanide position differs slightly for CLaNP-3, which may be caused by the differences in the structure between the two lanthanide probes. The correlation plots for the observed versus predicted distances, based on this position for the Gd^{3+} ion, show that distances of between 20 and 30 Å can be measured within an error margin of ±3 Å for both CLaNP-1–Paz and CLaNP-3–Paz (Figures 4B and C, respectively).

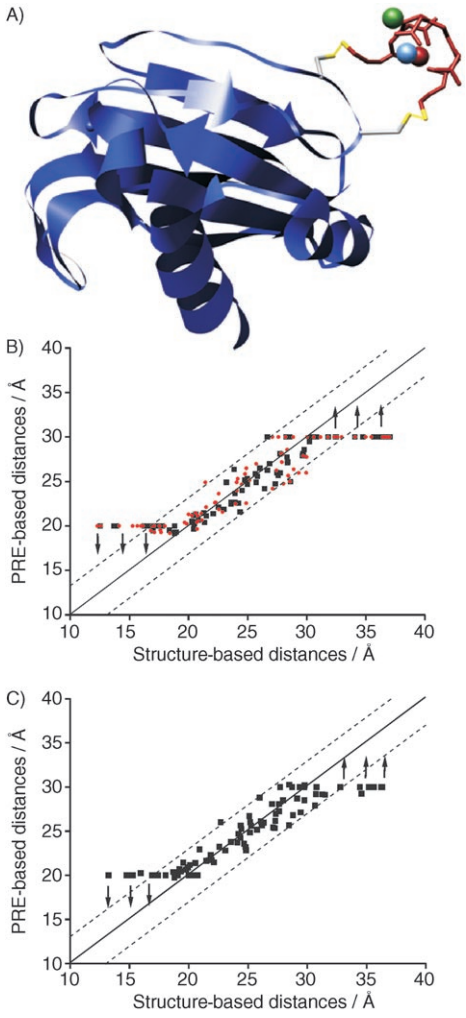

Figure 4. A) Optimized position of the Gd^{3+} in CLaNP-1–Paz (blue sphere) and in CLaNP-3–Paz (green sphere) are shown with respect to the position of Y^{3+} in CLaNP-1–Paz (red), taken from the crystal structure,[60] PDB entry 1PY0. The positions of the Gd^{3+} were generated in Xplor-NIH[78] by using the NMR distance restraints. B and C) Correlation between the observed and predicted Gd-to-H^N distances. Observed distances (PRE-based) were obtained from the NMR paramagnetic relaxation [Eq. (3)] of the Paz amides caused by the Gd^{3+} in CLaNP-1 (B) or CLaNP-3 (C). Predicted distances (structure-based) were determined by using the Xplor-generated positions of the Gd^{3+} in Paz–CLaNP (■) or the position of the lanthanide in the crystal structure of Paz–CLaNP-1 (●) (PDB entry 1PY0). The error-margin distances with 3 Å boundaries are marked by the dashed lines. The arrows pointing down and up emphasize that for some residues, only an upper or a lower experimental distance could be determined at 20 and 30 Å, respectively.

Conclusion

Paramagnetic effects can provide long-range-distance information that can be used in combination with other NMR-based restraints to determine the solution structure of proteins, global fold determination of larger proteins, and characterization of their different states. For applications to macromolecules that do not contain paramagnetic centers, paramagnetic surface tags can be employed. In this study, we present a new paramagnetic probe, covalently bound to a

protein in a bidentate fashion. The good agreement between observed and calculated PCS and PRE data indicates that the bidentate attachment helps to limit the conformational freedom of the metal relative to the protein. Thus, this probe can be used as a relaxation agent and, with some approximations, as a pseudocontact-shift agent, to obtain long-distance restraints for solving the solution structures of large proteins and protein–protein complexes. Such studies are currently in progress.

Experimental Section

Gadolinium(III) acetate (99.9%), yttrium(III) acetate (99.9%), ytterbium(III) nitrate, and the HBr salt of S-(2-methylaminomethyl)-methanesulfothioate (MTS) were used as purchased without further purification. Reactions were monitored by TLC analysis using DC-fertigfolien (Schleicher & Schuell, F1500, LS254) with detection by spraying with 20% H_2SO_4 in EtOH, $(NH_4)_6Mo_7O_{24}{\cdot}4H_2O$ (25 g L^{-1}), and $(NH_4)_4Ce(SO_4)_4{\cdot}2H_2O$ (10 g L^{-1}) in 10% sulfuric acid, or by spraying with a solution of ninhydrin (3 g L^{-1}) in EtOH/AcOH (20:1 v/v), followed by charring at ~150 °C. Column chromatography was performed on silica gel (0.04–0.063 mm) from Fluka. For LC-MS analysis (JASCO), an HPLC system (detection simultaneously at 214 and 254 nm) equipped with an analytical Alltima C_{18} column (4.6 mm × 250 mm, 5-μ particle size) was used in combination with buffers A: H_2O, B: MeCN, and C: 0.5% aq trifluoroacetic acid (TFA). Gradients of B were applied over 30 min, unless otherwise stated. Mass spectra were recorded by using a Perkin–Elmer Sciex API 165 equipped with a custom-made Electrospray Interface (ESI). Purifications were conducted by using a BioCAD "Vision" automated HPLC system (PerSeptive Biosystems), supplied with a semipreparative Alltima C18 column (5-μ particle size, running at 4 mL min^{-1}). Solvent system: A: 100% water, B: 100% acetonitrile, C: 1% TFA. Gradients of B in A containing 10% of C were applied over three column volumes (CV). ^{1}H NMR and ^{13}C NMR spectra were recorded by using a Bruker 200 MHz, a Bruker AV-400 (400/100 MHz), or a Bruker DMX-600 (600/150 MHz) spectrometer. Chemical shifts are given in ppm relative to tetramethylsilane (^{1}H NMR) as an internal standard or to the peak of the solvent used (^{13}C NMR).

CLaNP-3 synthesis

*1,7-Bis(*tert-*butyloxycarbonylmethylene)-4,10-bis(benzyloxycarbonylmethylene)-1,4,7,10-tetraazacyclododecano,* ***2***: Cyclen was converted into compound **1** as described previously.[65] Compound **1** (978 mg, 2.44 mmol) in CH_3CN (100 mL) and dry K_2CO_3 (4 g, 28.9 mmol) was treated dropwise with benzyl bromoacetate (0.8 mL, 5.0 mmol) under an argon atmosphere and stirring was continued for 48 h. The reaction mixture was filtered, concentrated, and purified by column chromatography (EtOAc:MeOH 9:1 + 2% TEA) to give compound **2** as a slightly yellow oil (480 mg, 28%). ^{1}H NMR (600 MHz, $CDCl_3$): δ = 7.41–7.26 (m, 10H; H_{ar}), 5.14, 4.70 (m, 4H; CH_2Ph), 3.85–3.66 (m, 8H; $CH_2C{=}O$), 3.35–2.84 (m, 16H; CH_2N), 1.53–1.26 ppm (m, 18H; $C(CH_3)_3$); ^{13}C NMR (150 MHz, $CDCl_3$): δ = 173.5, 173.0, 169.8, 168.9, 135.0, 134.9, 128.6, 128.5, 128.4, 128.3, 128.2, 127.4, 126.9, 82.6, 82.2, 66.9, 66.8, 65.0, 55.8, 55.7, 55. 4, 54.9, 51.5, 50.7, 46.1, 28.0, 27.9, 27.8, 8.7 ppm; MS (LC): *m*/*z*: 697.5 $[M+H]^+$ (10–90% buffer B; R_t 7.0 min); HRMS: *m*/*z*: calcd for $[C_{38}H_{56}N_4O_8+H]^+$: 697.4178; found: 697.4156.

*1,7-Bis(*tert-*butoxycarbonylmethylene)-1,4,7,10-tetraazacyclododecano-N″-N‴-bis(2′-(acetylamino)ethylmethanesulfonothioate)* ***3a***: Compound **2** (300 mg, 0.45 mmol) in degassed ethanol (8 mL) was treated with 10% palladium on carbon (16 mg) and then shaken under a hydrogen atmosphere (25 psi) for 48 h. The catalyst was removed with the aid of Hyflo, the filtrate was concentrated under reduced pressure, and traces of solvent were removed by using an oil pump. The residue was dissolved in chloroform (2 mL) by adding a small amount of DMF (0.05 mL) and the solution was added to a suspension of 2-(aminoethyl)methanethiosulfonate hydrobromide (222 mg, 0.94 mmol) in chloroform (2 mL) at 0 °C under an argon atmosphere in the presence of triethylamine (0.14 mL, 1.0 mmol) and HOBt (0.142 g, 1.05 mmol). EDCI (0.201 g, 1.05 mmol) was added to the reaction mixture and stirring was continued for 22 h at RT. The mixture was diluted with dichloromethane (15 mL) and was washed with HCl (10 mL, 0.5 M), satd aq $NaHCO_3$ (10 mL), and brine (10 mL). The organic phase was dried ($MgSO_4$), concentrated, and the residue was purified by repetitive RP-HPLC: flow rate 4.5 mL min^{-1}, step 0.5 CV; 10% buffer B followed by a linear gradient of 5.0 CV; 10–90% buffer B; R_t 1.5 CV, to give compound **3a** (90 mg, 26%) as a white, amorphous material after freeze-drying. ^{1}H NMR (600 MHz, CD_3CN): δ = 8.01, 7.65 (m, 2H; NH), 3.98–3.78 (m, 8H; $CH_2C{=}O$), 3.57–3.00 (m, 24H; $CH_2N + CH_2S$), 1.94 (s, 6H; CH_3SO_2), 1.47–1.43 ppm (m, 18H; $C(CH_3)_3$); ^{13}C NMR (50 MHz, CD_3CN): δ = 86.4, 86.2, 85.3, 84.5, 83.4, 56.0, 54.5, 52.5, 51.1, 49.3, 39.9, 36.2, 28.4 ppm; HRMS: *m*/*z*: calcd for $[C_{30}H_{58}N_6O_{10}S_4$ H$]^+$: 791.3177; found: 791.3188.

Lanthanide binding to 3b: Formation of the CLaNP-3 molecule: Compound **3a** (90 mg, 0.11 mmol) in CH_2Cl_2 (9 mL) was treated with TFA (4.5 mL) under an argon atmosphere at 0 °C. The reaction was complete after 5 h, as monitored by LC-MS. The mixture was concentrated under reduced pressure and the residue was purified by RP-HPLC: flow rate 4.5 mL min^{-1}, step 0.5 CV; 7% buffer B followed by a linear gradient of 3.0 CV; 7–16% buffer B; R_t 2.7 CV, yielding compound **3b** (28 mg, 36%) as a fluffy, white material after freeze-drying. A solution of compound **3b** in water (20 mM, pH ~2) was treated with the desired lanthanide salt in a 1:10 ratio and incubated for 24 h at 37 °C, followed by precipitation of the excess metal by increasing the pH to 9. The formation of the lanthanide-**3b** complex, from here on called CLaNP-3,[73] was monitored by LC-MS and ^{1}H NMR spectroscopy. The pH was immediately brought to 7 and CLaNP-3 was reacted with the protein (see below).

Protein production and purification: The expression plasmid containing the pseudoazurin gene of *Alcaligenes faecalis* S-6 and the mutagenesis of the residues 51 and 54 to cysteine, E51C/E54C, have been described previously.[60] The procedure for expression of the mutant gene in *Escherichia coli* BL21(DE3) cells was modified from that described previously.[60] The ^{15}N-labeled Paz E51C/E54C was obtained by culturing *E. coli* in M9 minimal medium containing $^{15}NH_4Cl$ as the sole nitrogen source (0.7 g L^{-1}) and kanamycin (50 mg L^{-1}). The cells were cultured at 30 °C until the OD_{600} reached 0.8, after which the temperature was lowered to 22 °C and, after 30 min, gene expression was induced with IPTG (0.5 mM). After 20 h of incubation at 22 °C, the culture was harvested by centrifugation. The cells were disrupted by sonication in buffer containing 20 mM sodium phosphate pH 7, NaCl (500 mM), phenylmethylsulfonyl fluoride (1 mM), DNase (50 μg mL^{-1}), and $CuCl_2$ (1 mM). Purification was performed according to a published protocol[60] to yield two fractions of pseudoazurin. These showed a single band on SDS-PAGE, however, the absorbance ratios of 275 nm over 593 nm were 2.2 and 1.8, respectively (a ratio of 1.9 was reported for the pure protein).[74] The latter (20 mg of Paz per L culture) was used in the NMR experiments.

Attachment of the CLaNP molecule to the Cu-containing E51C/E54C-Paz: Binding of CLaNP molecules to pseudoazurin through the two engineered Cys residues was performed as described,[60] but excluded the step of replacement of Paz cofactor with Zn. In short, the Paz-E51C/E54C mutant was incubated with DTT (5 mM) for 1 h at RT to dissociate the protein dimers. This was followed by removal of DTT on a desalting PD10 column equilibrated with degassed sodium phosphate buffer (20 mM, pH 7.0). Five molar equivalents of the probe molecule were added slowly to the protein solution and the reaction was left to proceed overnight at 4 °C under semianaerobic conditions. The protein-bound probe was then passed through a Superdex G75 column equilibrated with sodium phosphate buffer (20 mM, pH 7.0) containing NaCl (150 mM). Mass spectra analysis showed that almost all protein (>95%) treated in this way contained the bound probe.

NMR spectroscopy: The NMR samples of CLaNP–Paz (100–400μM) were prepared in sodium phosphate buffer (20 mM, pH 7) containing one equivalent of sodium ascorbate and 6% (v/v) D_2O. {^{1}H,^{15}N} HSQC experiments were acquired at 303 K by using a Bruker Avance DMX600 spectrometer. The spectral widths used were 32 and 12.6 ppm for the ^{15}N

and ^{1}H dimensions, respectively. The HSQC spectra were acquired with 2048 and 256 data points in t_2 and t_1, respectively. Data processing was performed by using the AZARA program (from http://www.bio.cam.ac.uk/azara) and the spectra were analyzed by using the program "Ansig for Windows".[75] The intensities of the crosspeaks were obtained by using parabolic peak fitting in the AZARA program. For resonances that were broadened beyond detection in the paramagnetic sample, an upper limit of the intensity was set by using the noise level. Assignments of the ^{1}H and ^{15}N amide nuclei of Cu(I)–Paz E51C/E54C were taken from previous work.[60,76]

Determination of the magnetic-susceptibility tensor: The pseudocontact shifts (δ^{pc}) caused by bonding of Yb^{3+} onto Paz were measured from the difference between the chemical shifts observed for the paramagnetic ^{Yb}CLaNP-3–Paz and the diamagnetic ^{Y}CLaNP-3–Paz. The size of the pseudocontact shift experienced by a nucleus under the influence of a paramagnetic center is described by Equation (1):

$$\delta^{pc} = \frac{1}{12\pi r^3}\left[\Delta\chi_{ax}(3\cos^2\theta - 1) + \frac{3}{2}\Delta\chi_{rh}(\sin^2\theta\cos 2\Omega)\right] \quad (1)$$

in which r, θ, and Ω are the polar coordinates of the nucleus with respect to the principal axes system of the magnetic-susceptibility tensor. $\Delta\chi_{ax}$ and $\Delta\chi_{rh}$ are the axial and rhombic anisotropy components of the magnetic-susceptibility tensor of the lanthanide ion, and are defined as $\Delta\chi_{ax} = \chi_{zz} - 0.5(\chi_{xx}+\chi_{yy})$ and $\Delta\chi_{rh} = \chi_{xx} - \chi_{yy}$, in which χ_{xx}, χ_{yy}, and χ_{zz} are the orthogonal components of the magnetic-susceptibility tensor. The apparent χ tensor was obtained by Euler rotation of the Gd-centered molecular coordinate frame and by fitting of the δ^{pc} values to Equation (1), according to the procedure described.[77] Proton coordinates were obtained by adding hydrogen atoms to the crystal structure of CLaNP-1–Paz (PDB entry 1PY0)[60] by using the programme Xplor-NIH.[78] The Gd^{3+} position relative to the Paz structure was that obtained after optimization by using ^{Gd}CLaNP-3-derived relaxation restraints (see below; the x, y, z coordinates of the Gd were 5.083, 14.480, 2.680 in the frame of 1PY0, respectively).

Pseudocontact shifts for 70 amide resonances were used in the calculation. For eight shifted resonances clearly showing split peaks in the ^{1}H dimension, an average δ^{pc} was used, with the distance to the mean as the error value. The Euler angles obtained for rotation of the Gd-centered coordinate frame into the χ tensor frame are $\alpha = 140° \pm 2$, $\beta = 112° \pm 1$, $\gamma = 100° \pm 6$, and $\Delta\chi_{ax} = 5.9(\pm 0.2)\times 10^{-32}\ m^3$, $\Delta\chi_{rh} = 1.9(\pm 0.4)\times 10^{-32}\ m^3$ (for $\Delta\chi_{ax} > \Delta\chi_{rh} > 0$).

PRE distances and optimization of the Gd positions: The intensity ratio of the amide resonances of the paramagnetic and diamagnetic form of the protein can be related to the paramagnetic contribution of the transverse ^{1}H relaxation according to Equation (2),[46] assuming that the contribution to the ^{15}N relaxation can be neglected:

$$\frac{I^{para}}{I^{dia}} = \frac{R_2^{dia}\exp(-R_2^{para}t)}{R_2^{dia} + R_2^{para}} \quad (2)$$

in which I^{para} and I^{dia} are the peak intensities for an amide resonance in the paramagnetic and diamagnetic sample, respectively; R_2^{dia} represents the intrinsic ^{1}H transverse relaxation rate, and t is the total INEPT evolution time of the signal (9 ms). R_2^{dia} is derived from the linewidths ($\Delta\nu_{1/2}$) of the resonances of the diamagnetic sample ($R_2^{dia} = \pi\Delta\nu_{1/2}$). To obtain $\Delta\nu_{1/2}$, the program MestRec (http://www.mestrec.com) was used, which allowed easy fitting and deconvolution of the partially overlapping peaks. In this way, more than 90% of the observed amide resonances could be used for distance-restraints calculations for both CLaNP molecules bound to the protein. The ^{1}H transverse-relaxation enhancements caused by the Gd^{3+}, R_2^{para}, were converted into distances by using Equation (3), which is a simplified version of the Solomon–Bloembergen equation:[72]

$$r = \sqrt[6]{\frac{1}{15}\left(\frac{\mu_0}{4\pi}\right)^2 \frac{\gamma_H^2 g^2 \mu_B^2 J(J+1)}{R_2^{para}}\left(4\tau_c + \frac{3\tau_c}{1+\omega_H^2\tau_c^2}\right)} \quad (3)$$

in which μ_0 is the vacuum permeability, γ_H is the proton gyromagnetic ratio, μ_B is the Bohr magneton, g is the electronic g factor, ω_H is the Larmor frequency of the proton spin, J is the quantum number for the Gd (7/2),[18] r is the lanthanide-to-amide proton distance in the protein, and τ_c is the total correlation time. The τ_c values were obtained from linear fits of R_2^{para} versus r^{-6} from the crystal structure of CLaNP-1–Paz.[60] Values of 4.0 and 5.9 ns were obtained for ^{Gd}CLaNP-1–Paz and ^{Gd}CLaNP-3–Paz, respectively.

The distances were separated into three classes of restraints. The first class comprised the residues for which the intensity of the amide resonances was affected more than five-fold. These residues were considered to be too close to the paramagnetic center for an accurate distance to be measured. A restraint with only an upper boundary of 20 Å was defined for these residues, which means they can be found anywhere up to 20 Å from the lanthanide. Given that the distance from the lanthanide ion in a CLaNP molecule to the nearest amide in the protein is about 8–9 Å, a "blind region" on the protein can be estimated by using this probe to be 11–12 Å. The second class contained the residues for which the intensity of the amide resonances was affected less than five-fold, but more than 1.2-fold. For these residues, a restraint to the experimental distance was defined with an upper and lower boundary of 3 Å. The third class comprised the residues for which the peak intensity was decreased less than 1.2-fold and these residues were considered to be too far away to be affected by the paramagnetic probe. To these residues, a restraint with only a lower boundary of 30 Å from the metal was defined. The number of restraints in each class is listed in Table 1.

Table 1. Number of restraints used in the Xplor-NIH distance calculations.

Probe attached to Paz	Upper boundary only	Lower boundary only	Upper and lower boundaries	Total restraints
^{Gd}CLaNP-1	12	19	49	80(87)[a]
^{Gd}CLaNP-3	13	14	59	86(90)[a]

[a] Total number of assigned residues in the spectra, including the residues for which overlapping resonances could not be used for an accurate linewidth determination.

The Gd^{3+} position with respect to the protein was determined through restrained energy minimization by using the program Xplor-NIH.[78] In these calculations, the protein was kept fixed (PDB, entry 1PY0),[60] and the Gd ion was allowed to move starting from ten random positions, solely under the influence of a distance-restraints energy term. This procedure yielded convergence to single positions for both CLaNP-1 and CLaNP-3 bound to Paz.

Acknowledgements

Dr J. A. Peters is acknowledged for careful reading of the manuscript. H. van den Elst and N. Meeuwenoord are thanked for their excellent HPLC and LC-MS assistance. M.D.V., M.P., and M.U. were supported by the Netherlands Organization for Scientific Research, VIDI-grant 700.52.425.

[1] M. Nomura, T. Kobayashi, T. Kohno, K. Fujiwara, T. Tenno, M. Shirakawa, I. Ishizaki, K. Yamamoto, T. Matsuyama, M. Mishima, C. Kojima, *FEBS Lett.* **2004**, *566*, 157–161.
[2] G. Otting, E. Liepinsh, K. Wuthrich, *J. Am. Chem. Soc.* **1991**, *113*, 4363–4364.
[3] C. M. Dobson, S. J. Ferguson, F. M. Poulsen, R. J. P. Williams, *Eur. J. Biochem.* **1978**, *92*, 99–103.
[4] G. Veglia, S. J. Opella, *J. Am. Chem. Soc.* **2000**, *122*, 11733–11734.

[5] E. Liepinsh, M. Baryshev, A. Sharipo, M. Ingelman-Sundberg, G. Otting, S. Mkrtchian, *Structure* **2001**, *9*, 457–471.
[6] S. Aime, N. D'Amelio, M. Fragai, Y. M. Lee, C. Luchinat, E. Terreno, G. Valensin, *J. Biol. Inorg. Chem.* **2002**, *7*, 617–622.
[7] G. Pintacuda, G. Otting, *J. Am. Chem. Soc.* **2002**, *124*, 372–373.
[8] S. Arumugam, C. L. Hemme, N. Yoshida, K. Suzuki, H. Nagase, M. Berjanskii, B. Wu, S. R. Van Doren, *Biochemistry* **1998**, *37*, 9650–9657.
[9] L. R. Dick, C. F. G. C. Geraldes, A. D. Sherry, C. W. Gray, D. M. Gray, *Biochemistry* **1989**, *28*, 7896–7904.
[10] M. Sattler, S. W. Fesik, *J. Am. Chem. Soc.* **1997**, *119*, 7885–7886.
[11] N. Niccolai, R. Spadaccini, M. Scarselli, A. Bernini, O. Crescenzi, O. Spiga, A. Ciutti, D. Di Maro, L. Bracci, C. Dalvit, P. A. Temussi, *Protein Sci.* **2001**, *10*, 1498–1507.
[12] A. M. Petros, L. Mueller, K. D. Kopple, *Biochemistry* **1990**, *29*, 10041–10048.
[13] M. Scarselli, A. Bernini, C. Segoni, H. Molinari, G. Esposito, A. M. Lesk, F. Laschi, P. Temussi, N. Niccolai, *J. Biomol. NMR* **1999**, *15*, 125–133.
[14] M. L. Deschamps, E. S. Pilka, J. R. Potts, I. D. Campbell, J. Boyd, *J. Biomol. NMR* **2005**, *31*, 155–160.
[15] N. Niccolai, O. Spiga, A. Bernini, M. Scarselli, A. Ciutti, I. Fiaschi, S. Chiellini, H. Molinari, P. A. Temussi, *J. Mol. Biol.* **2003**, *332*, 437–447.
[16] T. Yuan, H. Ouyang, H. J. Vogel, *J. Biol. Chem.* **1999**, *274*, 8411–8420.
[17] M. Sakakura, S. Noba, P. A. Luchette, I. Shimada, R. S. Prosser, *J. Am. Chem. Soc.* **2005**, *127*, 5826–5832.
[18] I. Bertini, C. Luchinat, G. Parigi, R. Pierattelli, *ChemBioChem* **2005**, *6*, 1536–1549.
[19] I. Bertini, A. Donaire, B. Jimenez, C. Luchinat, G. Parigi, M. Piccioli, L. Poggi, *J. Biomol. NMR* **2001**, *21*, 85–98.
[20] M. Allegrozzi, I. Bertini, M. B. L. Janik, Y. Lee, G. Liu, C. Luchinat, *J. Am. Chem. Soc.* **2000**, *122*, 4154–4161.
[21] I. Bertini, M. B. Janik, Y. M. Lee, C. Luchinat, A. Rosato, *J. Am. Chem. Soc.* **2001**, *123*, 4181–4188.
[22] M. Allegrozzi, I. Bertini, S. N. Choi, Y. M. Lee, C. Luchinat, *Eur. J. Inorg. Chem.* **2002**, 2121–2127.
[23] I. Baig, I. Bertini, C. Del Bianco, Y. K. Gupta, Y. M. Lee, C. Luchinat, A. Quattrone, *Biochemistry* **2004**, *43*, 5562–5573.
[24] R. Barbieri, I. Bertini, G. Cavallaro, Y. M. Lee, C. Luchinat, A. Rosato, *J. Am. Chem. Soc.* **2002**, *124*, 5581–5587.
[25] I. Bertini, C. Del Bianco, I. Gelis, N. Katsaros, C. Luchinat, G. Parigi, M. Peana, A. Provenzani, M. A. Zoroddu, *Proc. Natl. Acad. Sci. USA* **2004**, *101*, 6841–6846.
[26] R. R. Biekofsky, F. W. Muskett, J. M. Schmidt, S. R. Martin, J. P. Browne, P. M. Bayley, J. Feeney, *FEBS Lett.* **1999**, *460*, 519–526.
[27] M. A. Contreras, J. Ubach, O. Millet, J. Rizo, M. Pons, *J. Am. Chem. Soc.* **1999**, *121*, 8947–8948.
[28] G. L. Gay, D. A. Lindhout, B. D. Sykes, *Protein Sci.* **2004**, *13*, 640–651.
[29] D. F. Hansen, J. J. Led, *J. Am. Chem. Soc.* **2004**, *126*, 1247–1252.
[30] J. C. Hus, D. Marion, M. Blackledge, *J. Mol. Biol.* **2000**, *298*, 927–936.
[31] G. Pintacuda, K. Hohenthanner, G. Otting, N. Muller, *J. Biomol. NMR* **2003**, *27*, 115–132.
[32] G. Pintacuda, M. A. Keniry, T. Huber, A. Y. Park, N. E. Dixon, G. Otting, *J. Am. Chem. Soc.* **2004**, *126*, 2963–2970.
[33] J. R. Tolman, J. M. Flangan, M. A. Kennedy, J. H. Prestegard, *Proc. Natl. Acad. Sci. USA* **1995**, *92*, 9279–9283.
[34] J. T. Welch, W. R. Kearney, S. J. Franklin, *Proc. Natl. Acad. Sci. USA* **2003**, *100*, 3725–3730.
[35] P. B. Crowley, G. Otting, B. G. Schlarb-Ridley, G. W. Canters, M. Ubbink, *J. Am. Chem. Soc.* **2001**, *123*, 10444–10453.
[36] I. Díaz-Moreno, M. A. De la Rosa, M. Ubbink, *J. Biol. Chem.* **2005**, *280*, 18908–18915.
[37] M. Ubbink, M. Ejdebäck, B. G. Karlsson, D. S. Bendall, *Structure* **1998**, *6*, 323–335.
[38] C. Lange, T. Cornvik, I. Díaz-Moreno, M. Ubbink, *Biochim. Biophys. Acta* **2005**, *1707*, 179–188.
[39] D. F. Hansen, M. A. Hass, H. M. Christensen, J. Ulstrup, J. J. Led, *J. Am. Chem. Soc.* **2003**, *125*, 6858–6859.
[40] G. Pintacuda, A. Y. Park, M. A. Keniry, N. E. Dixon, G. Otting, *J. Am. Chem. Soc.* **2006**, *128*, 3696–3702.
[41] J. Feeney, B. Birdsall, A. F. Bradbury, R. R. Biekofsky, P. M. Bayley, *J. Biomol. NMR* **2001**, *21*, 41–48.
[42] V. Gaponenko, A. Dvoretsky, C. Walsby, B. M. Hoffman, P. R. Rosevear, *Biochemistry* **2000**, *39*, 15217–15224.
[43] C. Ma, S. J. Opella, *J. Magn. Reson.* **2000**, *146*, 381–384.
[44] J. Wohnert, K. J. Franz, M. Nitz, B. Imperiali, H. Schwalbe, *J. Am. Chem. Soc.* **2003**, *125*, 13338–13339.
[45] L. W. Donaldson, N. R. Skrynnikov, W. Y. Choy, D. R. Muhandiram, B. Sarkar, J. D. Forman-Kay, L. E. Kay, *J. Am. Chem. Soc.* **2001**, *123*, 9843–9847.
[46] J. L. Battiste, G. Wagner, *Biochemistry* **2000**, *39*, 5355–5365.
[47] V. Gaponenko, J. W. Howarth, L. Columbus, G. Gasmi-Seabrook, J. Yuan, W. L. Hubbell, P. R. Rosevear, *Protein Sci.* **2000**, *9*, 302–309.
[48] M. M. Dedmon, K. Lindorff-Larsen, J. Christodoulou, M. Vendruscolo, C. M. Dobson, *J. Am. Chem. Soc.* **2005**, *127*, 476–477.
[49] J. R. Gillespie, D. Shortle, *J. Mol. Biol.* **1997**, *268*, 158–169.
[50] S. U. Dunham, C. J. Turner, S. J. Lippard, *J. Am. Chem. Soc.* **1998**, *120*, 5395–5406.
[51] J. R. Gillespie, D. Shortle, *J. Mol. Biol.* **1997**, *268*, 170–184.
[52] A. Ramos, G. Varani, *J. Am. Chem. Soc.* **1998**, *120*, 10992–10993.
[53] K. Teilum, B. B. Kragelund, F. M. Poulsen, *J. Mol. Biol.* **2002**, *324*, 349–357.
[54] A. M. Petros, L. Mueller, K. D. Kopple, *Biochemistry* **1990**, *29*, 10041–10048.
[55] V. Gaponenko, A. S. Altieri, J. Li, R. A. Byrd, *J. Biomol. NMR* **2002**, *24*, 143–148.
[56] J. Iwahara, D. E. Anderson, E. C. Murphy, G. M. Clore, *J. Am. Chem. Soc.* **2003**, *125*, 6634–6635.
[57] A. Lewin, J. P. Hill, R. Boetzel, T. Georgiuo, R. James, C. Kleanthous, G. R. Moore, *Inorg. Chim. Acta* **2002**, *331*, 123–130.
[58] K. Tu, M. Gochin, *J. Am. Chem. Soc.* **1999**, *121*, 9276–9285.
[59] G. Pintacuda, A. Moshref, A. Leonchiks, A. Sharipo, G. Otting, *J. Biomol. NMR* **2004**, *29*, 351–361.
[60] M. Prudêncio, J. Rohovec, J. A. Peters, E. Tocheva, M. J. Boulanger, M. E. Murphy, H. J. Hupkes, W. Kosters, A. Impagliazzo, M. Ubbink, *Chem. Eur. J.* **2004**, *10*, 3252–3260.
[61] A. Dvoretsky, V. Gaponenko, P. R. Rosevear, *FEBS Lett.* **2002**, *528*, 189–192.
[62] A. Leonov, B. Voigt, F. Rodriguez-Castaneda, P. Sakhaii, C. Griesinger, *Chem. Eur. J.* **2005**, *11*, 3342–3348.
[63] V. Gaponenko, S. P. Sarma, A. S. Altieri, D. A. Horita, J. Li, R. A. Byrd, *J. Biomol. NMR* **2004**, *28*, 205–212.
[64] T. Ikegami, L. Verdier, P. Sakhaii, S. Grimme, B. Pescatore, K. Saxena, K. M. Fiebig, C. Griesinger, *J. Biomol. NMR* **2004**, *29*, 339–349.
[65] Z. Kovacs, A. D. Sherry, *Synthesis* **1997**, 759–763.
[66] S. Aime, M. Botta, M. Fasano, M. P. Marques, C. F. Geraldes, D. Pubanz, A. E. Merbach, *Inorg. Chem.* **1997**, *36*, 2059–2068.
[67] J. F. Desreux, *Inorg. Chem.* **1980**, *19*, 1319–1324.
[68] R. S. Ranganathan, N. Raju, H. Fan, X. Zhang, M. F. Tweedle, J. F. Desreux, V. Jacques, *Inorg. Chem.* **2002**, *41*, 6856–6866.
[69] Note that the PCS values expressed in Hz are different by a factor of ten for ^{1}H and ^{15}N, creating two exchange regimes for each residue. This makes it possible to observe two peaks in the ^{1}H dimension, with only a single resonance in the ^{15}N dimension. From these observations, the exchange rate (k_{ex}) is estimated to be $\sim 100\ s^{-1}$.
[70] S. Aime, A. Barge, M. Botta, M. Fasano, J. D. Ayala, G. Bombieri, *Inorg. Chim. Acta* **1996**, *246*, 423–429.
[71] V. Jacques, J. F. Desreux, *Inorg. Chem.* **1994**, *33*, 4048–4053.
[72] L. Banci, I. Bertini, C. Luchinat, *Nuclear and Electron Relaxation the Magnetic Nucleus-Unpaired Electron Coupling in Solution*, VCH, New York, NY, **1991**.

[73] We use the name CLaNP (Caged Lanthanide NMR Probe) to be consistent with earlier work. CLaNP-2 is an EDTA-based molecule with two functional groups for protein attachment. This molecule bound to proteins did not show sufficient Ln coordination.
[74] T. Kakutani, H. Watanabe, K. Arima, T. Beppu, *J. Biochem.* **1981**, *89*, 463–472.
[75] M. Helgstrand, P. Kraulis, P. Allard, T. Hard, *J. Biomol. NMR* **2000**, *18*, 329–336.
[76] A. Impagliazzo, M. Ubbink, *J. Biomol. NMR* **2004**, *29*, 541–542.
[77] J. A. Worrall, U. Kolczak, G. W. Canters, M. Ubbink, *Biochemistry* **2001**, *40*, 7069–7076.
[78] C. D. Schwieters, J. J. Kuszewski, N. Tjandra, G. M. Clore, *J. Magn. Reson.* **2003**, *160*, 65–73.

Received: June 27, 2006
Published online: November 20, 2006

